Proc. Int. Conf. Lasers '88, 594 (1989)

DIRECT VIBRATIONAL SPECTROSCOPY OF TRANSITION STATES

JACK A. SYAGE

Aerophysics Laboratory
P. O. Box 92957
The Aerospace Corporation
Los Angeles, CA 90009

Abstract

A technique for optically exciting and detecting vibrational resonances in transition state (TS) configurations of chemical reactions is described. By dressing the TS with intense infrared (IR) picosecond pulses (>GW/cm^2), for well-defined reactant initial conditions, resonant TS interactions such as absorption and stimulated emission can become manifested by measurable changes in the reaction rate and the product rovibrational distributions. In order that all TS configurations evolve during this pulse duration, a conventional pump-t-probe sequence using ultrashort pulses is used to initiate the reaction and to detect a product energy state after some time t that is short relative to the IR pulse duration. The transition states, therefore, evolve in an intense, but effectively continuous wave IR radiation field. The essential features illustrating the TS spectral lineshapes and experimental conditions were modeled by adopting a radiation-dressed potential surface and evaluating the vibrational transition probability by an exact density-matrix solution. Results are presented to describe, (1) the conditions under which significant TS transition probability occurs, and (2) how a frequency-resolved vibrational spectrum can be interpreted in terms of the detailed shape and dynamics of the reactive surface.

Introduction

During the course of a chemical reaction, a transformation of molecular bonds occurs which leads to structural configurations that are intermediate between reactants and products. These exceedingly short-lived structures have come to be known at "transition states". While it is true that the region known as the transition state can be rather diffuse and span a large configuration (or phase) space, the potential surface is believed to show ripples and shallow minima which can enhance the transient lifetimes of certain structures. The direct detection of transition states (or "reaction complexes") is considered one of the most important goals in chemistry and physics today.

One of the most fruitful approaches for obtaining transition state information has been to use crossed molecular beam systems to study the product angle-velocity distributions following monoenergetic collisional excitation.[1,2] State-to-state studies of reactant and product energy levels has also provided information that could be interpreted in terms of unique transition state properties.[2] The crossed beam and state-to-state experiments, however, do not directly observe the transition state, but rather derive detailed understanding via information obtained about the products.

Frequency-Domain Techniques: Brooks[3,4] and Polanyi[5,6] and their coworkers, using frequency-domain techniques, were the first to report evidence for spectroscopic detection of a transition state. The most compelling evidence by Brooks, *et al.*,[4] for TS absorption is an experiment based on the reaction K + NaCl + hν $\rightarrow$ KCl + Na*. They observed emission from the Na D line for hν excitation wavelengths that were off resonance from either reactant or product and concluded that the reaction complex [NaKCl]‡ must be the absorbing species. These wing absorptions in the reactive complex have the same physical basis as collisional line broadening. Polanyi focussed on a complementary approach, searching instead for wing emission eminating from the [FNaNa]‡ reactive complex. These early studies were marked by exceptionally weak signals that rendered analysis rather tenuous. Only since 1987 have major advances been made in the endeavor to detect transition states. Polanyi, *et al.*[6] have provided a convincing demonstration of detection, by multiphoton ionization, of a transient [HDD]‡ configuration in the exchange reaction H+D$_2$ $\rightarrow$ HD+D. However, the technique only probes for TS geometries that have Franck-Condon overlap with the excited and ionic bound states of HDD. This experiment has yet to resolve any resonances of [HDD]‡ from which to obtain structural and dynamical information. Valentini and Nieh[7] have recently reported the remarkable observation of collisional resonances in the H+H$_2$ reaction that correlate with enhanced production of H$_2$(v=1) averaged over all scattering angles. Although, not a direct observation, this result is, nonetheless, the most convincing measurement of vibrational structure in a TS. In another clever application, Neumark, *et al.*[8] formed stable anions of ClHCl$^-$ and then recorded photoelectron spectra to the unstable neutral complex ClHCl. The broad, but resolved spectrum is argued to represent vibrational information on the transition state region of the reaction Cl+HCl. The inevitable question regarding methods that rely on bound-unbound transitions, however, is to what extent the detected unbound geometry represents simply a Franck-Condon projections of the bound state.

Time-Domain Techniques: With continuing advances in ultrafast laser techniques, it is only natural that interest in time-domain techniques would ensue in the hunt for transition state detection. Zewail and coworkers have surged to the forefront in this endeavor with a number of important developments in 1987 and 1988.[9–11] Principal among these are results for the unimolecular

dissociation of ICN[9] and CH_3I[10] using a pump-t-probe scheme in which the probe frequency is tuned off-resonance of a reaction product. In so doing they observed signals that rise and fall with delay time t representing a transition state geometry that "passes through" a resonance with the probe frequency. The detection scheme is a variant of Brook's technique of using product emission to detect wing absorptions attributable to a collision complex. Instead, the reaction is unimolecular and initiated by a subpicosecond pulse. This has the advantage of providing very high instantaneous densities of transition state structures and the unquestioned benefits of time-resolved information. Using this same technique for the dissociation of NaI, Zewail and coworkers[11] have observed a periodicity in the formation of product Na due to a small nonadiabatic transition probability for reaction that occurs each time the vibrational motion of the excited NaI encounters a surface crossing transition region.

Transient Vibrational Spectroscopy

The optical detection of transition state configurations reported thus far have generated enormous excitement. However, there are still certain limitations to be overcome before they provide uniquely descriptive pictures of the transition state region. For instance, electronic transitions measure the energy difference between two different potential energy surfaces (PES); yet neither PES is likely to be known in the region of the transition state. Likewise, the use of bound-unbound transitions faces Franck-Condon restrictions that can severely limit the range of TS geometries that are actually detected.

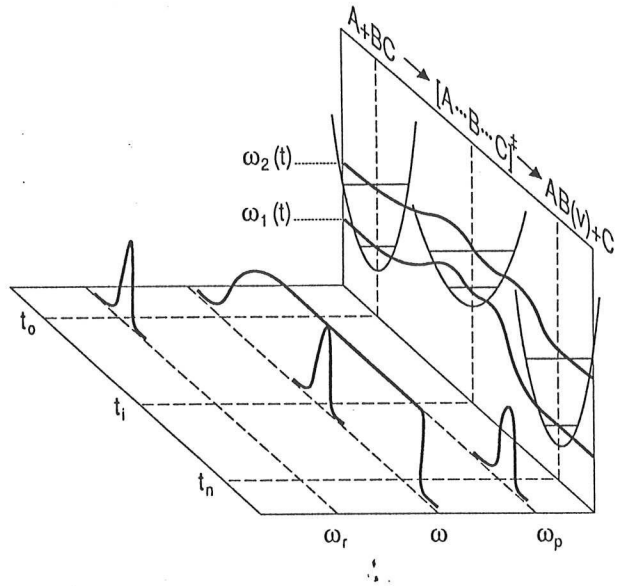

Fig. 1. Schematic of 3-pulse sequence for detecting vibrational resonances in transition states and reactive intermediate complexes. The pulses ω_r and ω_p refer to excitation of reactant and product, respectively. Idealized vibrationally adiabatic surfaces ($\omega_1(t)$ and $\omega_2(t)$) for the $[A\cdots B\cdots C]^{\ddagger}$ asymmetric stretch are drawn to correlate with reactant and product vibrations.

Concept of Experiment

We describe a technique that can provide vibrational spectra of transition states. The central idea here is that excitation of short-lived TS vibrations can become "imprinted" onto long-lived properties of the products (i.e., action spectroscopy) that can be routinely detected as a change in reaction probability or rate, and/or product rovibrational distribution. It has been recognized theoretically[12–14] that intense laser fields can interact with transition states and influence the course of a chemical reaction. The reactive-complex absorption wings, observed by Brooks[4] and Zewail[9–11] for electronic states, are an example of this phenomenon, in the sense that these absorptions produce electronically excited product. Work in this laboratory has shown that the conditions of a CW radiation dressed TS can be realized experimentally, in a manner that is sensitive to the detection of *vibrational resonances* in the TS.[15] The requirement of intense IR radiation (>GW/cm^2), during the course of the reaction, is satisfied by using short (e.g., picosecond) pulses. In order that all TS configurations evolve during this pulse duration, a conventional pump-t-probe sequence using ultrashort pulses is used to initiate the reaction and to detect a product energy state after some time t that is short relative to IR pulse duration. As represented schematically in Fig. 1, the presence of the ω long-pulse across the ω_r-τ-ω_p short-pulse interval describes a reaction that evolves in the presence of an intense CW radiation field.

Several modes of detecting TS vibrational resonances as a function of ω and τ can be envisioned to resolve the resonance frequencies, each providing unique details of the TS reactive PES and the coupling of vibrational energy to the reactive coordinate:

(1) Enhancement of reaction probability $P(\omega,\tau)$ or rate $k(\omega)$, due to TS absorption: This mode is particular sensitive if the excitation energy ω_r is below the reaction threshold.

(2) De-enhancement of $P(\omega,\tau)$ or $k(\omega)$, due to stimulated emission from collisionally excited TS vibrations: This variant would permit direct detection of the collisional resonances observed in molecular beam scattering experiments.[1,7]

(3) Excitation or de-excitation of product rovibrational energy corresponding to TS absorption or stimulated emission, respectively: The induced changes in the product state distributions can be correlated to the actual vibrational coordinates, amplitudes of motions, and angular momenta corresponding to the particular TS resonance.

(4) Ultrashort ω pulse that may be positioned within the reactive t period to probe early and late TS configurations. Exceptional time resolution ($\leq$ 100 fs) will be required, because the TS vibrational spectrum will be dominated by the most stable configuration.

The vibrational TS spectra are further enhanced by limiting the distribution of reactive trajectories so as to probe specific regions of transitional configuration space. This can be achieved by studying unimolecular reactions, or oriented bimolecular reactions initiated by dissociating a molecule in a suitably chosen van der Waals mixed dimer[16] (e.g., $XA\cdot BC \xrightarrow[-X]{} [A\cdots B\cdots C]^{\dagger} \rightarrow AB + C$). A quantitative model for establishing the necessary experimental conditions, as well as interpreting the TS vibrational lineshapes, is presented later.

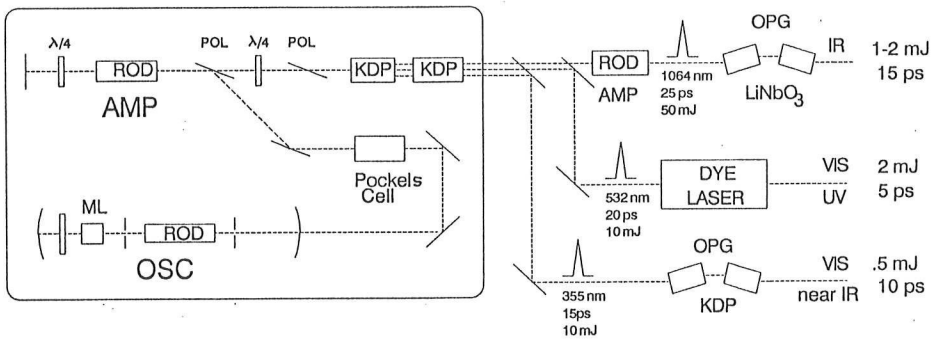

Fig. 2. Schematic for generating 3-pulse sequence, using a pulsed mode-locked (ML) Nd:YAG laser, short-cavity dye laser, and optical parametric generation (OPG) devices. Typical pulse energies and durations are indicated.

Experimental Arrangement

The three-pulse sequence diagrammed in Fig. 1 will be generated by a picosecond Nd:YAG laser pumping a combination of tunable optical parametric devices and a tunable ps dye laser. An arrangement, which makes use of the Nd:YAG fundamental (1064 nm) and the second (532 nm) and third harmonics (355 nm) is given in Fig. 2. Our approach takes maximum advantage of the high pulse energies provided by our pulsed and amplified mode-locked laser. Typical pulse energies and pulsewidths in the standard configuration are included in Fig. 2 for each stage leading to the three pulses, ω_r, ω, and ω_p.

The source of vibrational excitation in the transition state will take the form of 15-20 ps tunable IR pulses of about 1-2 mJ/pulse. This is generated by a standard nonlinear parametric method[17] which uses the intense 1064 nm Nd:YAG pulse to generate two sum frequencies in the IR with a tuning range of 1.5-5 μm. Modest focussing to beam diameters less than 1 mm gives the necessary > 10 GW/cm^2 pulse energies to vibrationally excite TS configurations. The pump (ω_r) and probe (ω) pulses require a large visible (VIS) and ultraviolet (UV) tuning range. This is provided by a short-cavity dye laser, pumped by the 532 nm Nd:YAG output. A second source of tunable visible frequencies is available by pumping an optical parametric arrangement with the 355 nm Nd:YAG harmonic.

Theoretical Description

In this section, we provide the beginnings of a quantitative basis for interpreting the TS spectra. The model calculations to follow not only demonstrate the soundness of the experimental approach, but make the physical connection between observed spectra and the detailed dynamics of a collision complex on a reactive potential surface.

The Photon-Dressed Potential Energy Surface

The essential features illustrating vibrational correlation, TS spectral lineshapes, and experimental conditions can be viewed by adopting a simple model for a radiatively dressed PES and evaluating the transition probability by an exact density matrix solution. This is an appropriate representation because the intense IR pulse ω appears as a constant radiation field over the short detected reaction period t, as illustrated in Fig. 1. For vibrational excitation on the same electronic surface, the Hamiltonian (in frequency units) may be written as

$$\begin{aligned} \mathcal{H} &= \mathcal{H}_o(t) + \mathcal{H}_{int}(t) \\ \mathcal{H}_o &= T_q + \omega a^+ a^- \\ \mathcal{H}_{int} &= \mu(t) \cdot \epsilon_o (a^+ + a^-) \end{aligned} \tag{1}$$

$\mathcal{H}_o$ consists of the nuclear kinetic energy operator T_q and the field-free radiation Hamiltonian where a^+ and a^- are the photon creation and annihilation operators. The interaction Hamiltonian $\mathcal{H}_{int}$ contain the dipole operator μ and laser electric field strength ϵ_o (we assume a single mode and polarization). Operation of $\mathcal{H}$ on the matter-radiation basis states gives the diagonal energy matrix elements,

$$\begin{aligned} \langle n, \chi_1 | \mathcal{H}_o(t) | \chi_1, n \rangle &= \omega_1(t) + \omega \\ \langle n-1, \chi_2 | \mathcal{H}_o(t) | \chi_2, n-1 \rangle &= \omega_2(t) \end{aligned} \tag{2a}$$

where $|n\rangle$ and $|n-1\rangle$ are the photon states in an n-photon field (where we consider only one-photon transitions). The interaction of the dipole moment with the incident radiation field has only the off-diagonal elements

$$\langle n, \chi_1 | \mathcal{H}_{int}(t) | \chi_2, n-1 \rangle = \langle n-1, \chi_2 | \mathcal{H}_{int}(t) | \chi_1, n \rangle = \frac{\mu(t)\epsilon_o}{2} \tag{2b}$$

The time dependence arises from the effect of the reactive trajectory velocity vector $v(r,t)$ on the coordinate dependent Hamiltonian. The radiation-dressed lower surface is shifted from the uncoupled surface (given by $T_q|\chi_1\rangle = \omega_1|\chi_1\rangle$) by the radiation frequency ω. If the dressed lower surface approaches or crosses the upper surface then, depending on the interaction strength $\mu\epsilon_o$, a mixing of states occurs which makes possible a transition.

The mixing of the basis states gives the correct shape of the PES in the vicinity of the crossing. The true eigenfunctions $|\chi'\rangle$ and energies η' can be solved for the time-dependent Hamiltonian elements above, and are given by

$$\begin{aligned} |\chi_1'\rangle &= |\chi_1\rangle \cos\theta + |\chi_2\rangle \sin\theta \\ |\chi_2'\rangle &= -|\chi_1\rangle \sin\theta + |\chi_2\rangle \cos\theta \end{aligned} \tag{3}$$

where

$$\begin{aligned} \tan 2\theta &= \frac{\mu(t)\epsilon_o}{\Omega(t)} \\ \eta'_{1,2} &= \pm[\mu(t)^2\epsilon_o^2 + \Omega(t)^2]^{1/2} \\ \Omega &= (\omega_2 - \omega_1) - \omega \end{aligned}$$

Rotation Matrix Solution

We find it advantageous to use the density matrix formalism for evaluating population probabilities or densities. The time-dependent probability of populating the upper level can be evaluated by solving the density matrix equation $\dot{\rho} = i[\rho, H]$ for the element ρ_{22}. This formalism has the advantage of leading to a solution that is completely general for all models of the PES surface and interaction strengths. Without presenting the full details[15] here, we solve for the four elements of ρ by casting them as a column vector and applying an appropriate transformation[18] to help decouple the equations. One obtains, .

$$\begin{aligned} \hat{\rho}(t_n) &= \mathcal{R}(t_n, t_o)\hat{\rho}(t_o) \\ \mathcal{R}(t_n, t_o) &= \exp\left\{ i \int_{t_o}^{t_n} \mathcal{L}(t) dt \right\} \end{aligned} \tag{4}$$

where $\hat{\rho}$ is the column vector $\{\rho_{11}-\rho_{22};\, i(\rho_{12}-\rho_{21});\, \rho_{12}+\rho_{21}\}$ and $\mathcal{L}$ follows from the transformed equations $\frac{d}{dt}\hat{\rho} = i\mathcal{L}\hat{\rho}$. The evaluation of the evolution operator $\mathcal{R}(t_n, t_o)$ is essentially intractable except for the simplest Hamiltonian time dependences. However, in the appropriate representation,[18] $\mathcal{R}(t_n, t_o)$ takes the form of a rotation matrix that can be expressed conveniently by a piecewise product of rotation matrices

$$\mathcal{R}(t_n, t_o) = \mathcal{R}(t_n, t_{n-1}) \cdots \mathcal{R}(t_1, t_o) \tag{5}$$

over incremental time intervals during which $\mathcal{H}$ is approximately constant. The coherence properties and their intermediate role in the time-evolved transition probability are fully preserved by this treatment.

The vibrational transition probability at the end of a reactive trajectory is evaluated by solving for the population difference $\rho_{11} - \rho_{22}$. For the initial condition $\rho_{12}(t_o) = \rho_{21}(t_o) = 0$, the r_{11} element of the product matrix $\mathcal{R}(t_n, t_o)$ must be evaluated. The product of matrices in Eq. (5) can be reduced to a product of 2x2 matrices $\mathcal{Q}(t_n, t_o) = \prod_{i=1}^{n} \mathcal{Q}(t_i, t_{i-1})$ consisting of the elements

$$\begin{aligned} q_{11}(\tau_i) &= q_{22}^*(\tau_i) = \cos\frac{1}{2}\bar{b}_i\tau_i - i\cos\theta_i \sin\frac{1}{2}\bar{b}_i\tau_i \\ q_{12}(\tau_i) &= q_{21}(\tau_i) = i\sin\theta_i \sin\frac{1}{2}\bar{b}_i\tau_i \end{aligned} \tag{6}$$

with terms defined as

$$\begin{aligned} \tan\theta_i &= \frac{\bar{\Omega}_i}{\bar{\mu}_i\epsilon_o} \\ \Omega(t) &= \omega_2(t) - \omega_1(t) - \omega \\ b(t) &= \left[\mu(t)^2\epsilon_o^2 + \Omega(t)^2\right]^{1/2} \end{aligned}$$

where $\tau_i = t_i - t_{i-1}$ and the bar represents the average value over the τ_i interval. The general solution for $\Delta\rho = \rho_{11} - \rho_{22}$ is then given by

$$\Delta\rho(t_n) = r_{11}(t_n, t_o)\Delta\rho(t_o) \tag{7}$$

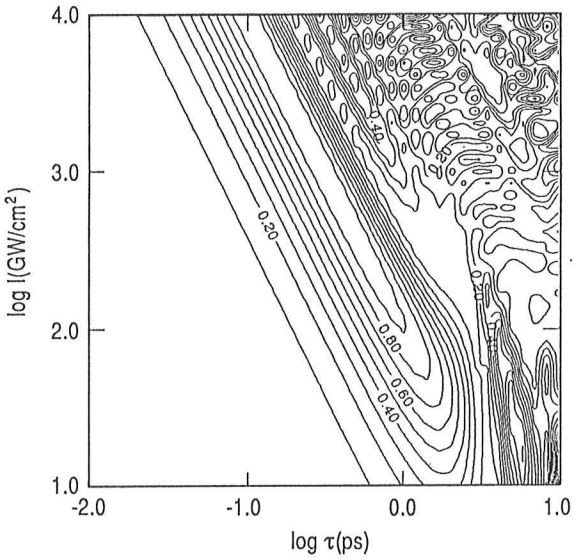

Fig. 3. Transition probability $P(v, v+1)$ for absorption ($\Delta\rho(t_o) = 1$) or stimulated emission ($\Delta\rho(t_o) = -1$) as a function of laser power density and quasibound lifetime τ. Parameters used in the contour plot were $\mu(t) = 0.2$ D, $\omega = 2020$ cm^{-1}, and $\omega_k(t) = a_k[(2t/\tau) - 1]^2 + b_k$ where $a_1 = 80$ cm^{-1}, $b_1 = 1000$ cm^{-1}, and $a_2 = 160$ cm^{-1}, $b_2 = 3000$ cm^{-1}.

where $r_{11}(t_n, t_o)$ is obtained from the elements of the product matrix $\mathcal{Q}(t_n, t_o)$ by the expression

$$r_{11} = \frac{1}{2}[(q_{11}^2 + q_{22}^2) - (q_{12}^2 + q_{21}^2)] \tag{8}$$

Model Calculations

The above model will serve to demonstrate the experimental technique represented in Fig. 1 by addressing two important questions; (1) under what conditions will a significant TS transition probability occur, and (2) can a frequency-resolved vibrational spectrum be interpreted in terms of the detailed shape and dynamics of the reactive PES? These points are examined in Figs. 3-5. Although, we shall use a general strong-field, coherent density matrix solution, we adopt a simple model for the reactive trajectory in that we assume localized trajectories, no decay or relaxation processes other than reaction, and simple functional forms for the potential surfaces.

The calculated results are based on a shallow potential well in the TS region for a particular vibrational coordinate on the ground electronic surface. We assume parabolic well depths of 0.01 eV and 0.02 eV for the vibrational levels v and $v+1$, and a dipole moment of 0.2 D. These values are consistent with [FHF]† in the F+HF reaction. Transition probabilities $P(v, v+1)$ are calculated as a function of IR laser power density I ($\epsilon_o \propto I^{1/2}$), and trajectory time through this region (i.e., quasibound lifetime τ). We assume that regions outside of the well are vanishingly short-lived.

The results in Fig. 3 indicate that significant values of $P(v, v+1)$ occur over a range of modest experimental conditions. For instance, $P(v, v+1) > 0.25$ for $I = 100$ GW/cm^2 and $\tau > 300$ fs. The oscillations that are observed along τ (shown

bunched up due to the log scale) are analogous to Rabi cycling, which for resonance conditions occurs at frequency $\mu\epsilon_o$. For dynamic trajectories, the resonance condition is rapidly detuned by the changing potentials, however, phase accumulation can still lead to off-resonance oscillations provided that $\mu\epsilon_o \geq \Omega$. In realistic systems, the coherences will dampen rapidly either by (i) T_2 mechanisms, in which case the oscillation region reduces to the saturation condition $P = 0.5$, or by (ii) very different v and $v + 1$ quasibound lifetimes, in which case the shorter-lived state will behave irreversibly, making possible situations approaching $P = 1$.

The bandshape for the TS vibrational transition $v \rightarrow v + 1$ is calculated for excitation over the entire quasibound lifetime in Fig. 4. The spectrum reveals a distinct lineshape that does not change form as a function of laser field. The spectra are therefore interpretable in terms of the shape and dynamics of the transient vibrational potential; power broadening, at the high fields shown, does not contribute to the lineshape.

Fig. 4 represents the experiment in which the the IR pulse duration is long compared to the reaction time so that all TS configurations evolve in an intense, but effectively CW laser field. An exceptionally more powerful (and more challenging) adaptation can be conceived based on the use of ultrashort pulses (e.g., $\leq$ 200 fs) that are narrower than the quasibound lifetimes. The ω pulse can then be positioned at discrete intermediate time intervals along the reactive trajectory and in principle probe for different TS configurations. The recorded vibrational spectra will vary depending on where along the reactive PES the excitation takes place. This concept is similar to the 2-pulse sequence introduced by Zewail and coworkers[9-11] for electronic transitions in product absorption wings. The calculated time-dependent vibrational spectrum in Fig. 5 demonstrates the considerable detail and unique information that can be obtained regarding the dynamics and shape of the potential surfaces. The two-dimensional (ω, t) vibrational spectrum in Fig. 5 represents the direct change in vibrational frequency that occurs during a reactive trajectory.

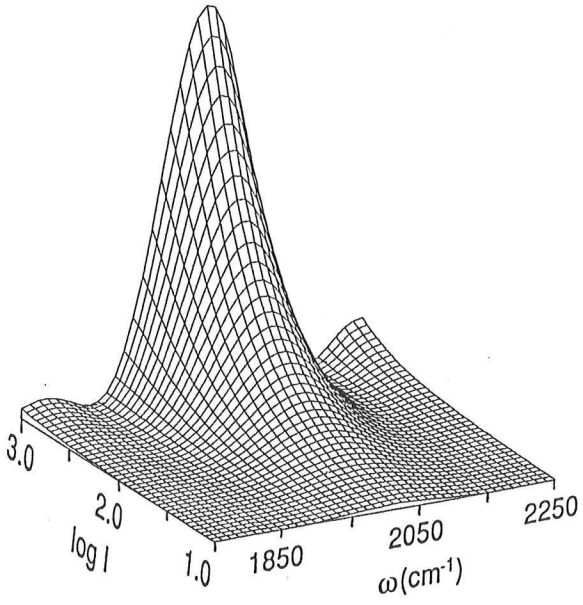

Fig. 4. Calculated transition state vibrational lineshapes. Continuous excitation over a trajectory liftime of 250 fs. Peak transition probability was $P = 0.89$ Other conditions were $I = 100$ GW/cm^2 and those in the caption to Fig. 3.

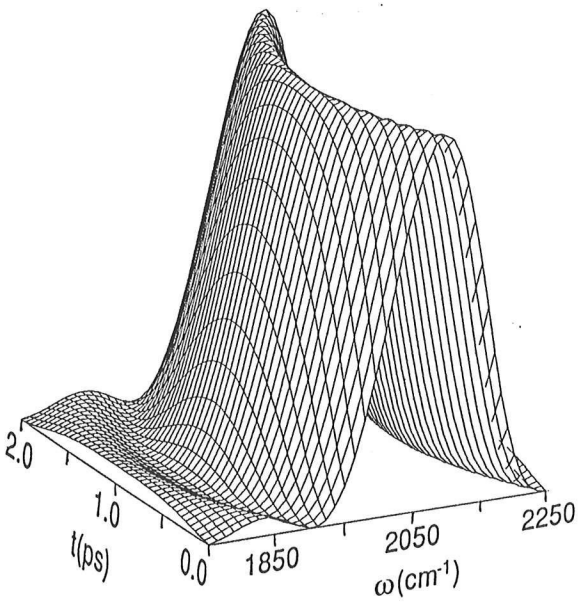

Fig. 5. Calculated transition state vibrational lineshapes. Discrete excitation over 200 fs intervals as a function of time during a reactive trajectory of lifetime 2 ps. Peak probability was $P = 0.10$. Other conditions were $I = 100$ GW/cm^2 and those in the caption to Fig. 3.

Vibrational Correlation

The transition-state vibrational absorption technique described here is, in a sense, a state-to-state measurement, with the important difference that we consider state excitation of the TS. The correlation of TS vibrational excitation to measurable rovibrational excitation in the products is a "half collision" process that is physically not unlike that which occurs in unimolecular dissociations. Using this as an analogy, we can put forth a framework for the state-to-state half-collision reaction probabilities for vibrationally-excited TS reactions $[ABC(v')]^{\ddagger} \rightarrow AB(v)+C$. In order to present expressions that convey physical insight, we simplify the problem by invoking the collinear and quasi-diatomic approximations. The former assumption is realistic in so far as the minimum reactive PES is usually along the collinear coordinate in the complete reactive hypersurface. The latter approximation assumes that the bond that breaks is a normal vibrational coordinate. The state-to-state reaction probability $T_{v'v}$ is then given by the integral overlap of the initial and final wavefunctions

$$T_{v'v} = \iint dR dr \; \chi_{v'}(R,r)\chi_v(R,r) \qquad (9)$$

where we have defined the coordinates R and r as the internuclear distances A-B and B-C, respectively. The wavefunctions χ describe vibrational and translational motion and can be rigorously solved by Schrodinger's equations using a Hamiltonian contain-

ing the relative nuclear kinetic energy operators evaluated at the critical TS coordinate. The Hamiltonian may also be modified by including a dressed photon field in the manner described above. The product wavefunctions are expanded in terms of a basis of vibrational functions $\phi_{v,j}(R,r)$ with an r-dependent equilibrium position R_o,

$$\chi_v(R,r) = \sum_j \phi_{v,j}(R,r)\alpha_j(r) \tag{10}$$

The coefficients $\alpha_j(r)$ are related to the relative product translational energy. Inserting Eq. (10) into Eq. (9) gives the final result

$$T_{v'v} = \sum_j S_{v',j}F_{j,v} \tag{11}$$

where

$$F_{j,v} = \iint dRdr\ \chi_{v'}(R,r)\phi_{v,j}(R,r) \tag{12a}$$

$$S_{v',j} = \int dr\ \chi_{v'}(R,r)\alpha_j(r) \tag{12b}$$

The half-collision state-to-state reaction probability given by Eqs. (11) and (12) reveals two possible mechanisms for final-state distributions; the $F_{j,v}$ terms [Eq. (12a)] describe the Franck-Condon contributions, while the $S_{v',j}$ terms [Eq. (12b)] represent the half-collision analog of the S matrix in scattering theory. The $S_{v',j}$ matrix elements describe the so-called final-state interactions, which considers product vibrational excitation due to the dynamics of the repulsive surface in the exit channel. Although, final-state interactions play an important role, experimental[2,19] and theoretical[20,21] evidence indicates that the product state distributions are most strongly affected by the multi-dimensional Franck-Condon factors. These results support the strong role that vibrational correlation can play in the interpretation of product rovibrational excitation in terms of the actual vibrational coordinates, amplitudes of motion, and angular momenta corresponding to a particular TS resonance.

References

1. D. M. Neumark, A. M. Wodtke, G. N. Robinson, C. C. Hayden and Y. T. Lee, *J. Chem. Phys.*, **82**, 3045 (1985); D. M. Neumark, A. M. Wodtke, G. N. Robinson, C. C. Hayden and Y. T. Lee, Phys. Rev. Lett., **53**, 226 (1984).

2. R. B. Bernstein, *Chemical Dynamics via Molecular Beam and Laser Techniques* (Oxford University Press, New York, 1982).

3. P. Hering, P. R. Brooks, R. F. Curl, R. S. Judson and R. S. Lowe, *Phys. Rev. Lett.*, 44, 687 (1980); P. R. Brooks, R. F. Curl and T. C. Maguire, *Ber. Bunsenges. Phys. Chem.*, **86**, 401 (1982).

4. T. C. Maguire, P. R. Brooks, R. F. Curl, J. H. Spence, and S. J. Ulvick, *J. Chem. Phys.* **85**, 844 (1986).

5. P. Arrowsmith, S. H. P. Bly, P. E. Charters and J. C. Polanyi, *J. Chem. Phys.*, **79**, 283 (1983); J. C. Polanyi and R. J. Wolf, *J. Chem. Phys.*, **75**, 5951 (1981).

6. B. A. Collings, J. C. Polanyi, M. A. Smith, A. Stolow, and A. W. Tarr, *Phys. Rev. Lett.* **59**, 2551 (1987).

7. J-C. Nieh and J. J. Valentini, *Phys. Rev. Lett.* **60**, 519 (1988).

8. R. B. Metz, T. Kitsopoulos, A. Weaver, and D. M. Neumark, *J. Chem. Phys.* **88**, 1463 (1988).

9. M. Dantus, M. J. Rosker, and A. H. Zewail, *J. Chem. Phys.* **87**, 2395 (1987).

10. L. R. Khundkar and A. H. Zewail, *Chem. Phys. Lett.* **142**, 426 (1987).

11. T. S. Rose, M. J. Rosker, and A. H. Zewail, *J. Chem. Phys.* **88**, 6672 (1988).

12. J-M. Yuan and T. F. George, *J. Chem. Phys.* **68**, 3040 (1978); K-S. Lam and T. F. George, *J. Chem. Phys.* **76**, 3396 (1982).

13. A. M. F. Lau, *Phys. Rev. A* **16**, 1535 (1977); A. M. F. Lau and C. K. Rhodes, *Phys. Rev. A* **15**, 1570 (1977); J. Jiang and J. S. Hutchinson, *J. Chem. Phys.* **87**, 6973 (1987); J. C. Light, *J. Chem. Phys.* **66**, 5241 (1977).

14. A. E. Orel and W. H. Miller, *J. Chem. Phys.*. **70**, 4393 (1979); *ibid*, **72**, 5139 (1979); *ibid*, **73**, 241 (1980)

15. J. A. Syage, *Phys. Rev. Lett.*, submitted

16. S. Buelow, M. Noble, G. Radhakrishnan, H. Reisler, C. Wittig, and G. Hancock, *J. Phys. Chem.* **90**, 1015 (1986); G. Radhakrishnan, S. Buelow, and C. Wittig, *J. Chem. Phys.* **84**, 727 (1986).

17. A. Laubereau and W. Kaiser, *Rev. Mod. Phys.* **50**, 607 (1978); A. Seilmeier, K. Spanner, A. Laubereau, and W. Kaiser, *Optics Commun.* **24**, 237 (1978)

18. R. P. Feynman, F. L. Vernon, and R. W. Hellwarth, *J. Appl. Phys.* **28**, 49 (1957).

19. J. C. Polanyi, *Science* **236**, 680 (1987).

20. R. H. Bisseling, P. L. Gertitschke, R. Kosloff, J. Manz, *J. Chem. Phys.* **88**, 6193 (1988); R. H. Bisseling, R. Kosloff, J. Manz, *J. Chem. Phys.* **83**, 993 (1985).

21. K. F. Freed and Y. B. Band, in *Excited States, Vol. 3*, edited by E. C. Lim, (Academic, New York, 1977) p. 109; V. Halavee and M. Shapiro, *Chem. Phys.* **21**, 105 (1977); G. C. Schatz and J. Ross, *J. Chem. Phys.* **66**, 1021, 1037 (1977).